ELSEVIER

Journal of Fluids and Structures 20 (2005) 763–783

JOURNAL OF FLUIDS AND STRUCTURES

www.elsevier.com/locate/jfs

Parametric resonances of supported pipes conveying pulsating fluid

J.D. Jin*, Z.Y. Song

Department of Aeronautical and Astronautical Engineering, Shenyang Institute of Aeronautical Engineering, Shenyang 110034, P.R. China

Received 3 September 2003; accepted 2 April 2005
Available online 1 July 2005

Abstract

In this paper, the stability and parametric resonances of supported pipes conveying pulsating fluid are studied via numerical methods. According to the stability criterion derived, the effect of physical parameters of the system on the regions of three parametric resonances is discussed. The amplitude–frequency response curves of the parametric resonances and their frequency characteristics are investigated through numerical simulations. The results obtained show that several motions can take place in the region of combination resonance, including quasiperiodic and combined periodic motions. There exist some regions of overlap between the regions of the different resonances, and hence different types of steady state response may occur at the same value of the exciting frequency ω in these regions of overlap. This phenomenon may lead to sudden changes in motion from one steady state response to another.

Keywords: Supported pipes; Parametric resonance; Stability

1. Introduction

Pipes conveying steady flow may lose stability by divergence but cannot undergo oscillatory type instabilities (flutter) if they are supported (pinned or clamped) at both ends (Holmes, 1978). However, a harmonically fluctuating flow may cause the pipes to undergo another type of dynamic instability due to parametric resonances (Païdoussis, 1998). Contributions on this problem include the works of Chen (1971), Ginsberg (1973), Païdoussis and Issid (1974), Païdoussis and Sundararajan (1975), Ariaratnam and Namachchivaya (1986), etc. in the framework of linear analysis. Experiments were conducted by Païdoussis and Issid (1976). Using the method of averaging, nonlinear analysis was performed for the same problem by Namachchivaya (1989) and Namachchivaya and Tien (1989a,b). In these nonlinear analyses the detuning of frequency, which describes the nearness of the exciting frequency to the frequency of resonance, is a small parameter used in the method of averaging, and so their analytical solutions obtained are valid only in a neighborhood of the resonances. Therefore, it would be of interest to investigate how far the regions of the parametric vibrations can extend away from the resonance regions, and what behavior would occur in the regions of nonresonance.

*Corresponding author.
E-mail address: jinjd@163.com (J.D. Jin).

0889-9746/$ - see front matter © 2005 Elsevier Ltd. All rights reserved.
doi:10.1016/j.jfluidstructs.2005.04.007

In this paper, we analyze numerically the parametric resonances of the supported pipes conveying pulsating fluid. The influence of the various parameters of the system on the regions of parametric resonance is investigated according to the analytical expressions of stability boundaries derived. The amplitude–frequency curves of the parametric resonances are studied through tracing the resonance curves numerically, with varying the exciting frequency from the region of resonance to that of nonresonance.

2. Differential equation of motion and discretization

The systems considered are shown in Fig. 1.The pinned–pinned and clamped–clamped pipes conveying fluid are considered to be vertical and to be subject to planar motions: $y(x,t)$. The pipe axis in the undeformed state coincides with the x-axis, which is in the direction of gravity. The nonlinear terms considered here are only the additional axial force induced by lateral motions of the pipes. Such a nonlinear equation of motion, given by Holmes (1977), is

$$\left(1+a\frac{\partial}{\partial t}\right)EI\frac{\partial^4 y}{\partial x^4}+\left\{MU^2-\overline{T}+\overline{PA}(1-2v)-\left[(M+m)g-M\frac{\partial U}{\partial t}\right](L-x)\right\}\frac{\partial^2 y}{\partial x^2}$$
$$-\left[\left(1+a\frac{\partial}{\partial t}\right)\frac{E\widetilde{A}}{2L}\int_0^L\left(\frac{\partial y}{\partial x}\right)^2\mathrm{d}x\right]\frac{\partial^2 y}{\partial x^2}+(M+m)\frac{\partial^2 y}{\partial t^2}+2MU\frac{\partial^2 y}{\partial x\partial t}+(M+m)g\frac{\partial y}{\partial x}=0, \tag{1}$$

where EI is the flexural rigidity of the pipes, a the coefficient of Kelvin-Voigt viscoelastic damping of the pipe material, v the Poisson ratio, $\widetilde{A}$ the cross-sectional area of the pipe wall, g the acceleration due to gravity, $\overline{T}$ static tension in the pipe, L the pipe length, and m its mass per unit length; M is the mass of the fluid conveyed per unit length, $\overline{A}$ the cross-sectional flow area and U flow velocity in the pipe, and $\overline{P}$ the internal pressure at $x=L$. Since the internal pressurization, $\overline{P}$, merely adds an additional constant tensile force to the external tension, $\overline{T}$, one can take $\overline{P}=0$ (Holmes, 1977).

Introducing the following nondimensional variables and parameters:

$$\eta=\frac{y}{L},\quad \xi=\frac{x}{L},\quad \bar{g}=\frac{M+m}{EI}L^3 g,\quad \bar{\tau}=\left(\frac{EI}{M+m}\right)^{1/2}\frac{t}{L^2},\quad u=\left(\frac{M}{EI}\right)^{1/2}LU, \tag{2}$$

$$M_r=\left(\frac{M}{M+m}\right)^{1/2},\quad \alpha=\left(\frac{EI}{M+m}\right)^{1/2}\frac{a}{L^2},\quad T=\frac{\overline{T}L^2}{EI},\quad \gamma=\frac{\widetilde{A}L^2}{2I},$$

Eq. (1) may be written in dimensionless form as

$$\alpha\dot{\eta}''''+\eta''''+[u^2-T+(M_r\dot{u}-\bar{g})(1-\xi)-\gamma\int_0^1(\eta')^2\,\mathrm{d}\xi-2\alpha\gamma\int_0^1\eta'\dot{\eta}'\,\mathrm{d}\xi]\eta''$$
$$\ddot{\eta}+2M_r u\dot{\eta}'+\bar{g}\eta'=0, \tag{3}$$

where $()'$ and $\dot{()}$ denote $\partial()/\partial\xi$ and $\partial()/\partial\bar{\tau}$, respectively. The fluid velocity is assumed to be harmonically fluctuating and to have the following dimensionless form:

$$u=u_0(1+\mu\cos(\omega\bar{\tau})), \tag{4}$$

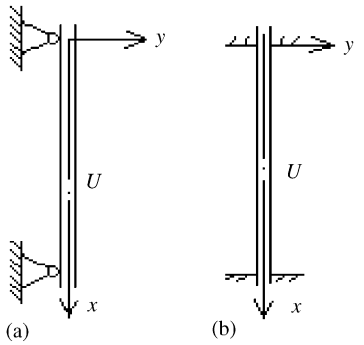

Fig. 1. Schematic of the system treated in this paper: (a) pinned–pinned pipe; (b) clamped–clamped pipe.

where u_0 is the mean flow velocity, μ is the amplitude of the harmonic fluctuation (assumed small) and ω is its frequency. Substituting Eq. (4) into Eq. (3) yields

$$\ddot{\eta} + 2M_r u_0 \dot{\eta}' + \dot{\eta}'''' + \eta'''' + [u_0^2 - T - \bar{g}]\eta'' + \bar{g}\xi\eta'' + \bar{g}\eta' = \mu[M_r u_0 \omega(1-\xi)\eta'' \sin(\omega\bar{\tau}) - (2u_0^2\eta'' + 2M_r u_0 \dot{\eta}')\cos(\omega\bar{\tau})] + \gamma\eta'' \int_0^1 (\eta')^2 \,\mathrm{d}\xi + 2\alpha\gamma\eta'' \int_0^1 \eta'\dot{\eta}' \,\mathrm{d}\xi. \tag{5}$$

Note that in Eq. (5) the higher-order terms of μ have been omitted.

To discretize Eq. (5) in accordance with Galerkin's method, let

$$\eta(\xi, \bar{\tau}) = \sum_{i=1}^{N} \psi_i(\xi) q_i(\bar{\tau}), \tag{6}$$

where $q_i(\bar{\tau})$, $i = 1, 2, \ldots, N$, are the generalized coordinates and $\psi_i(\xi)$are the eigenfunctions of the supported (pinned–pinned or clamped-clamped) beam. It was pointed out by Païdoussis and Issid (1974) that the instability boundaries for pinned-pinned and clamped-clamped pipes could be determined with the two-mode expansion ($N = 2$) of Eq. (6) with adequate precision, and their experimental results were found to be at least in good qualitative agreement with those predicted by theory (Païdoussis and Issid, 1976). As the main purpose of this paper is to investigate some of the qualitative behavior of the system, a two-mode expansion ($N = 2$) of Eq. (6) is taken in the analytical model for simplicity. Substituting Eq. (6) for $N = 2$ into Eq. (5) and employing the orthogonality property of the modes, one can reduce the partial differential Eq. (5) after laborious calculation to a four-dimensional first–order ordinary differential equation:

$$\dot{\mathbf{z}} = \mathbf{S}\mathbf{z} + \mu\omega\mathbf{B}_1\mathbf{z}\sin(\omega\bar{\tau}) - \mu\mathbf{B}_2\mathbf{z}\cos(\omega\bar{\tau}) - \alpha\mathbf{B}_3\mathbf{z} - \mathbf{Q}(\mathbf{z}), \tag{7}$$

where

$$\mathbf{z} = (q_1, q_2, q_3, q_4)^{\mathrm{T}}, \quad q_3 = \dot{q}_1, \quad q_4 = \dot{q}_2, \quad \alpha \equiv \mu\bar{\alpha},$$

$$\mathbf{S} = \begin{pmatrix} \mathbf{O} & \mathbf{I} \\ \overline{\mathbf{S}}_1 & \overline{\mathbf{S}}_2 \end{pmatrix}, \quad \mathbf{B}_1 = M_r u_0 \begin{pmatrix} \mathbf{O} & \mathbf{O} \\ \overline{\mathbf{B}}_1 & \mathbf{O} \end{pmatrix}, \quad \mathbf{B}_2 = \begin{pmatrix} \mathbf{O} & \mathbf{O} \\ \overline{\mathbf{B}}_2 & -\overline{\mathbf{S}}_2 \end{pmatrix}, \quad \mathbf{B}_3 = \begin{pmatrix} \mathbf{O} & \mathbf{O} \\ \mathbf{O} & \overline{\mathbf{B}}_3 \end{pmatrix},$$

$$\overline{\mathbf{S}}_1 = \begin{pmatrix} -\lambda_1^4 - c_{11}\beta & -\bar{g}e_{12} \\ -\bar{g}e_{12} & -\lambda_2^4 - c_{22}\beta \end{pmatrix}, \quad \overline{\mathbf{S}}_2 = \begin{pmatrix} 0 & 2M_r u_0 b_{21} \\ -2M_r u_0 b_{21} & 0 \end{pmatrix}, \quad \mathbf{O} = \begin{pmatrix} 0 & 0 \\ 0 & 0 \end{pmatrix},$$

$$\mathbf{I} = \begin{pmatrix} 1 & 0 \\ 0 & 1 \end{pmatrix}, \quad \overline{\mathbf{B}}_1 = \begin{pmatrix} c_{11}/2 & -b_{21} - e_{12} \\ b_{21} - e_{12} & c_{22}/2 \end{pmatrix}, \quad \overline{\mathbf{B}}_2 = \begin{pmatrix} 2c_{11}u_0^2 & 0 \\ 0 & 2c_{22}u_0^2 \end{pmatrix}, \quad \overline{\mathbf{B}}_3 = \begin{pmatrix} \lambda_1^4 & 0 \\ 0 & \lambda_2^4 \end{pmatrix},$$

$$\beta = u_0^2 - T - \tfrac{1}{2}\bar{g}, \quad \mathbf{Q}(\mathbf{z}) = (0, 0, Q_1, Q_2)^{\mathrm{T}}, \quad (Q_1, Q_2)^{\mathrm{T}} = F_{\mathrm{T}}(q_1 c_{11},\ q_2 c_{22})^{\mathrm{T}},$$

$$F_T = \gamma c_{11}(q_1^2 + 2\alpha q_1 q_3) + \gamma c_{22}(q_2^2 + 2\alpha q_2 q_4). \tag{8}$$

Depending on the end conditions of the pipe, different values should be taken for some parameters in the above expressions. For the pinned-pinned pipe, we have

$$\lambda_1 = \pi, \quad \lambda_2 = 2\pi, \quad b_{21} = 8/3, \quad c_{11} = -\pi^2, \quad c_{22} = -4\pi^2, \quad e_{12} = 40/9,$$

for the clamped-clamped pipe, we have

$$\lambda_1 = 4.730040745, \quad \lambda_2 = 7.853204624, \quad b_{21} = 3.342015505, \quad c_{11} = -12.302617073,$$
$$c_{22} = -46.050128937, \quad e_{12} = 3.342619181.$$

3. Averaged equations and regions of parametric resonances

The eigenvalue problem of $\mathbf{S}$ yields a quartic characteristic equation of the form

$$\omega_i^4 + p_1\omega_i^2 + p_2 = 0, \tag{9}$$

where

$$p_1 = \beta(c_{11} + c_{22}) + \lambda_1^4 + \lambda_2^4 + 4M_r^2 u_0^2 b_{21}^2,$$
$$p_2 = c_{11}c_{22}\beta^2 + (c_{22}\lambda_1^4 + c_{11}\lambda_2^4)\beta + \lambda_1^4\lambda_2^4 - \bar{g}e_{12}^2,$$
$$p_3 \equiv p_1^2 - 4p_2. \tag{10}$$

Numerical analysis shows that for small mean velocity of flow below the critical velocity, u_c corresponding to divergence instability of the pipe, we always have $p_1 > 0$, $p_2 > 0$ and $p_3 > 0$. Hence, for $u_0 < u_c$ the matrix $\mathbf{S}$ always has two pairs of pure imaginary eigenvalues: $\pm i\omega_1$, $\pm i\omega_2$ ($i = \sqrt{-1}$), where ω_1 and ω_2 are the undamped natural frequencies of the first and second modes of the system. We consider in this paper only the case of $u_0 < u_c$; that is, we consider only the parametric resonances which take place from a stable state of the pipe.

The matrix $\mathbf{S}$ can be put into Jordan normal form by a transformation matrix $\mathbf{V}$ which is composed of the eigenvectors of $\mathbf{S}$. Now we introduce the transformations

$$\mathbf{z} = \sqrt{\mu}\,\mathbf{V}\mathbf{x} \text{ and } \tau = \omega\bar{\tau},$$

and substitute them into Eq. (7) to obtain

$$\dot{\mathbf{x}} = \frac{\mathbf{\Omega}}{\omega}\mathbf{x} + \mu\left[\left(\mathbf{A}_1 \sin\tau - \frac{1}{\omega}\mathbf{A}_2 \cos\tau - \frac{\bar{\alpha}}{\omega}\mathbf{A}_3\right)\mathbf{x} - \frac{\mathbf{f}(\mathbf{x})}{\omega}\right], \tag{11}$$

where

$$\mathbf{x} = (x_1, x_2, x_3, x_4)^{\mathrm{T}}, \quad \mathbf{\Omega} = \mathbf{V}^{-1}\mathbf{S}\mathbf{V}, \quad \mathbf{A}_i = \mathbf{V}^{-1}\mathbf{B}_i\mathbf{V}\ (i = 1, 2, 3), \quad \mathbf{f}(\mathbf{x}) = \mathbf{V}^{-1}\mathbf{Q}(\mathbf{V}\mathbf{x}). \tag{12}$$

In Eqs. (11) and (12) we have used the fact that the nonlinear terms in $\mathbf{Q}(\mathbf{z})$ are all cubic with respect to $\mathbf{z}$.

Next, we introduce the detuning parameter λ through

$$\omega = \omega_0(1 + \lambda), \tag{13}$$

λ being small and having the form of $\lambda = \mu\bar{\lambda}$. This implies that the analysis to be carried out is valid only in the neighborhood of some given frequency ω_0. Applying the method of averaging one can derive the following three regions of parametric resonance by using a similar technique as developed by Ariaratnam and Namachchivaya (1986).

3.1. For $\frac{\omega_1}{\omega_0} = \frac{1}{2}$

In this case we have

$$\left|\omega/\omega_1 - 2\right| < \left\{\mu^2\left(U_1^2 + V_1^2\right) - \left[\alpha\Lambda_1/\omega_1\right]^2\right\}^{1/2}, \tag{14}$$

where

$$U_1 = A_1^{22} - A_1^{11} - (A_2^{12} + A_2^{21})/\omega_0, \quad V_1 = A_1^{12} + A_1^{21} + (A_2^{22} - A_2^{11})/\omega_0, \quad \Lambda_1 = A_3^{11} + A_3^{22}. \tag{15}$$

In the above expressions, A_s^{ij} denotes the element of the matrix $\mathbf{A}_s (s = 1, 2, 3)$ with ith row and jth column. The pipe loses stability in this region by the parametric resonance, and we will refer to the motions as the first mode (sub-harmonic) parametric resonance in what follows.

3.2. For $\frac{\omega_2}{\omega_0} = \frac{1}{2}$

In this case

$$|\omega/\omega_2 - 2| < \left\{\mu^2(U_2^2 + V_2^2) - [\alpha\Lambda_2/\omega_2]^2\right\}^{1/2}, \tag{16}$$

where

$$U_2 = A_1^{44} - A_1^{33} - (A_2^{34} + A_2^{43})/\omega_0, \quad V_2 = A_1^{34} + A_1^{43} + (A_2^{44} - A_2^{33})/\omega_0, \quad \Lambda_2 = A_3^{33} + A_3^{44}. \tag{17}$$

Sub-harmonic oscillations occur in this region and we will refer to the motions as the second mode (sub-harmonic) parametric resonance.

3.3. For $\dfrac{\omega_1+\omega_2}{\omega_0}=1$

In this case

$$\lambda^2\Lambda_1\Lambda_2<(\Lambda_1+\Lambda_2)^2[\mu^2B/16-\alpha^2\Lambda_1\Lambda_2/(4\omega_0^2)], \tag{18}$$

where

$$\begin{aligned} &U_{12}=A_1^{24}-A_1^{13}-(A_2^{14}+A_2^{23})/\omega_0, \quad V_{12}=A_1^{14}+A_1^{23}+(A_2^{24}-A_2^{13})/\omega_0, \quad B=U_{12}U_{21}+V_{12}V_{21},\\ &U_{21}=A_1^{42}-A_1^{31}-(A_2^{41}+A_2^{32})/\omega_0, \quad V_{21}=A_1^{41}+A_1^{32}+(A_2^{42}-A_2^{31})/\omega_0. \end{aligned} \tag{19}$$

The pipe loses stability in this region and develops quasiperiodic oscillations with two basic frequencies. We refer to the motions as the combination (parametric) resonances in what follows.

The reader is referred to Appendix A for details for deriving the boundary equations of various resonance regions.

4. Effect of parameters on the regions of parametric resonances

In this section, we discuss the effect of the parameters of the system on the regions of parametric resonances. In Figs. 2(a) and (b), three regions of parametric resonances, determined by the expressions of Eqs. (14), (16) and (18), are shown for pinned-pinned and clamped-clamped pipes, respectively. In each of Figs. 2a and b, the regions in the left and right sides correspond to the parametric resonances of the first and second modes, respectively, and the middle one is the combination resonance. These three resonance regions are located near $\omega_0=2\omega_1$, $\omega_0=\omega_1+\omega_2$ and $\omega_0=2\omega_2$, respectively, in both pipes. The parameter values applied in Fig. 2 were chosen to be (Namachchivaya, 1989; Namachchivaya and Tien, 1989a):

$$u_0=1.88, \quad M_r=0.8, \quad \alpha=0.005, \quad \overline{g}=T=0 \tag{20}$$

for the pinned-pinned pipe, and

$$u_0=4.0, \quad M_r=0.447, \quad \alpha=0.001, \overline{g}=T=0 \tag{21}$$

for the clamped–clamped pipe. In the following analysis of this section the same parameter values will be taken as shown in Eqs. (20) and (21), except for those parameters that are given with special values other than above. In Figs. 3(a)–(j) the effects of some parameters, such as the damping (α), mean flow velocity (u_0), mass ratio (M_r), tension (T) and gravity ($\overline{g}$), on the resonance regions are shown. As we see from Figs. 3(a) and (b), with increasing α the resonance regions are displaced upwards and hence for a given value of μ, the range of ω where the resonances occur becomes narrower. As the mean flow velocity, u_0, is increased the regions of parametric resonance are displaced towards the left of the figure, which reflects the fact that the natural frequencies of the first and second modes of the system decrease with increasing flow velocity, as shown in Figs. 3(c) and (d) . It can also be seen from the figures that the regions of these instabilities are displaced downwards and become broader with increasing u_0; this implies that as the mean flow velocity

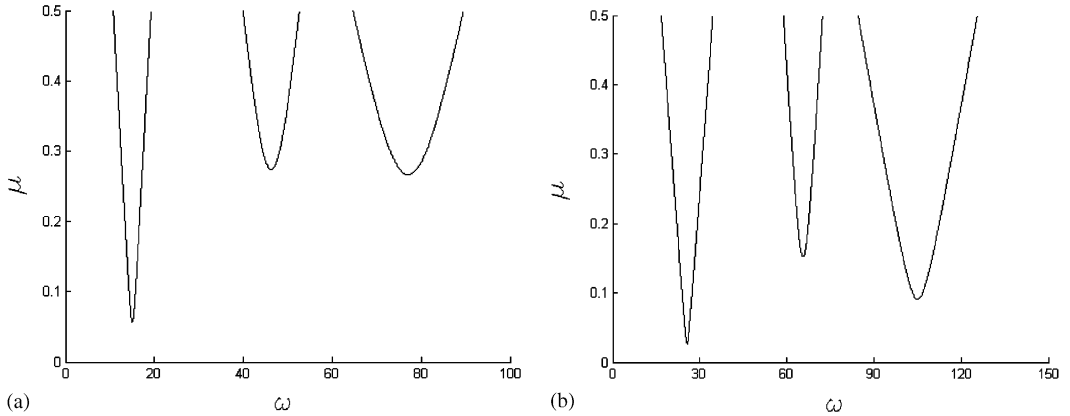

Fig. 2. The regions of the three parametric resonances: (a) pinned–pinned pipe ($u_0=1.88, M_r=0.8, \alpha=0.005, \overline{g}=T=0$); (b) clamped–clamped pipe ($u_0=4.0, M_r=0.447, \alpha=0.001, \overline{g}=T=0$).

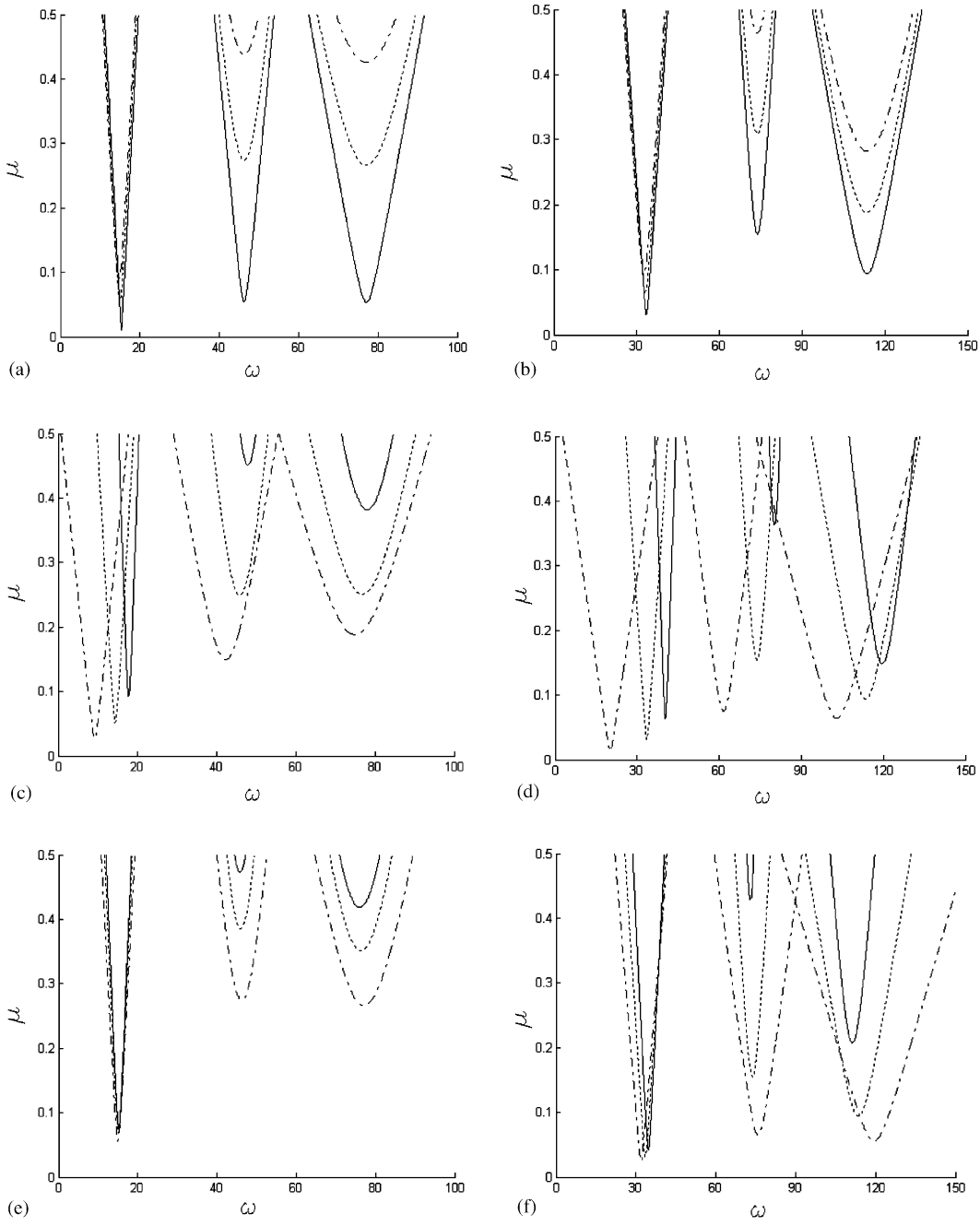

Fig. 3. The effect of various parameters on the regions of parametric resonance. (a) Effect of damping for a pinned–pinned pipe, for $\alpha = 0.001,\ 0.005,\ 0.008$. In this figure, and in what follows, we indicate the curves corresponding to the first, second and third parameter values by a solid, dotted and dash–dot lines, respectively. (b) Effect of damping for a clamped–clamped pipe for $\alpha = 0.001,\ 0.002,\ 0.003$. (c) Effect of mean velocity for a pinned-pinned pipe for $u_0 = 1.3,\ 2.0,\ 2.7$. (d) Effect of mean velocity for a clamped-clamped pipe for $u_0 = 2.5,\ 4.0,\ 5.6$. (e) Effect of mass ratio for a pinned-pinned pipe for $M_r = 0.5,\ 0.6,\ 0.8$. (f) Effect of mass ratio for a clamped-clamped pipe for $M_r = 0.2,\ 0.447,\ 0.8$. (g) Effect of tension for a pinned-pinned pipe for $T = -5,\ 0,\ 10$. (h) Effect of tension for a clamped-clamped pipe for $T = -15,\ 0,\ 20$. (i) Effect of gravity for a pinned-pinned pipe for $\bar{g} = -10,\ 0,\ 15$. (j) Effect of gravity for a clamped-clamped pipe for $\bar{g} = -20,\ 0,\ 30$.

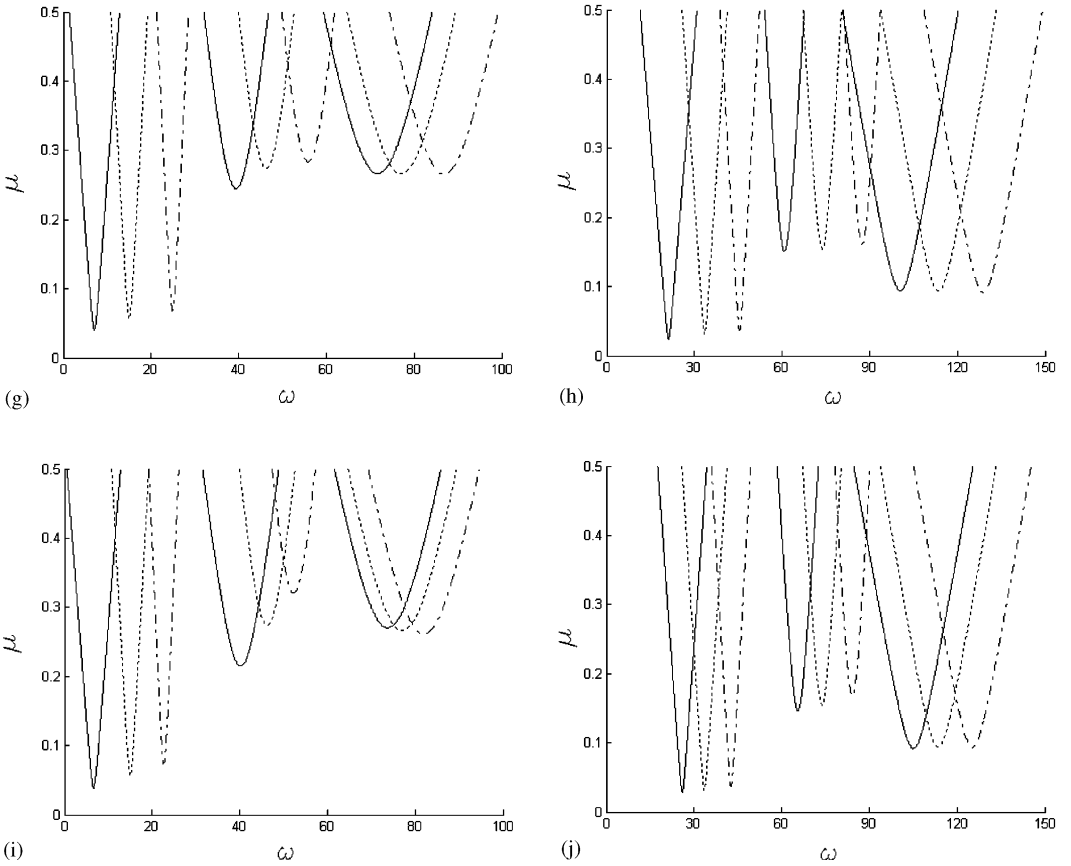

Fig. 3. (*Continued*)

is increased the system loses its stability more easily with the smaller amplitude of excitation and with the broader range of excitation frequency ω. Figs. 3(e) and (f) show the effect of the mass ratio, M_r, on the regions of parametric resonances. With increasing M_r, the resonance regions become broader, and are displaced downwards in the direction of the μ-axis; whereas in the direction of the ω-axis different trends are observed depending on the different parametric resonances. The region of first-mode resonance is displaced towards the left with increasing M_r; while the regions of second-mode and combination resonances are displaced towards the right, which reflect the fact that the natural frequency of the first mode decreases somewhat with increasing M_r, while the frequency of the second mode increases with increase of M_r [cf. Païdoussis and Issid (1974, Fig. 3)].

The effect of the tension (T) and gravity ($\overline{g}$) on the regions of parametric resonance is shown in Figs. 3(g), 3(h) and 3(i), 3(j). As T is increased the resonance regions are displaced towards the right of the figure, which reflects the increase of the natural frequencies of both the first and second modes with increasing T; while in the direction of the μ-axis the resonance regions almost have no change of location, except that the regions of the first mode resonance and combination resonance for the pinned-pinned pipe are displaced upwards slightly with increasing T. As $\overline{g}$ is increased ($\overline{g}<0$ represents the flow moves upwards, i.e., in the opposite direction to the gravity) the resonance regions are also displaced towards the right since the natural frequencies of the first and second modes increase with increasing $\overline{g}$, and a similar effect is to be found as is seen when T is increased. The effect of some parameters on the stability region were discussed in the work of Païdoussis and Issid (1974), Païdoussis and Sundararajan (1975) and Ariaratnam and Namachchivaya (1986); the results in this paper are in good agreement with these earlier results. Comparison of the boundary equations for instability (resonance) between the result obtained by Ariaratnam and Namachchivaya (1986) and the result of this paper is made in Appendix A, and the two results are found to be equivalent in fact.

In Fig. 4, the boundaries of instability given in the present paper are compared with those given in previous study by Païdoussis and Issid (1974) for a clamped-clamped pipe as M_r and α are varied, and it is found that most of these results are in good agreement except for some cases when $\alpha = 0$. In Fig. 4(a), these two results are compared for $M_r = 0.2$ and

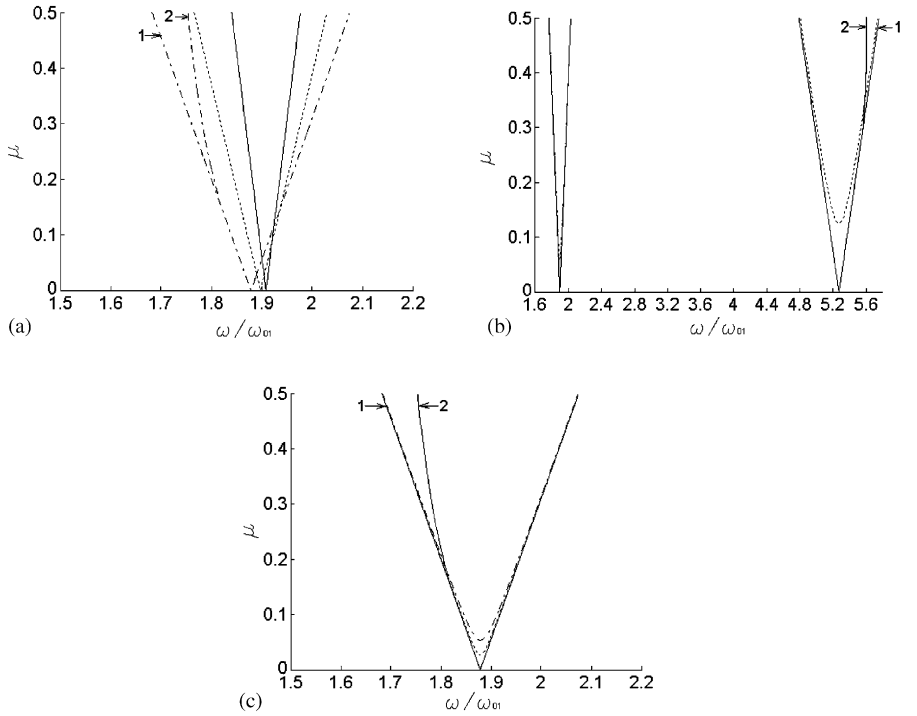

Fig. 4. Comparison of the boundaries of instability from the present results to those of previous investigations by Païdoussis and Issid (1974) for a clamped–clamped pipe. In the figures, ω_{01} represents the first mode natural frequency at zero flow. (a) The regions of the first mode resonance for $M_r = 0.2, 0.5, 0.8$ ($u_0 = 2, \alpha = 0, \bar{g} = 10, T = 0$). The two results are in agreement for $M_r = 0.2$ and 0.5. For $M_r = 0.8$, the left boundaries in the two results are in disagreement; 1, present result; 2, Païdoussis and Issid (1974). (b) The regions of the first and second mode resonances for $\alpha = 0$ and 0.000754 ($u_0 = 2, M_r = 0.5, \bar{g} = 10, T = 0$). For $\alpha \neq 0$, the boundaries in the two results are in agreement. For $\alpha = 0$, the right boundaries of the second mode resonance in the two results are in disagreement; 1, present result; 2, Païdoussis and Issid (1974). (c) The instability boundaries for the same system as in Fig. 4(a) for $M_r = 0.8$ and for $\alpha = 0$, 0.0005, 0.001; 1, present result (for $\alpha = 0$); 2, Païdoussis and Issid (1974) (for $\alpha = 0$).

0.5 and found to be almost identical, and hence the difference in boundaries in these two results is not discernible in the figure. However, for $M_r = 0.8$, though the right boundaries are in good agreement, the left boundaries are in disagreement since the boundary in previous investigation by Paidoussis and Issid (1974) (see Fig. 12 in their paper) is not straight. In Fig. 4(b), the boundaries of instability in the two results are found to be in good agreement for $\alpha \neq 0$; while for $\alpha = 0$, the right boundaries of the second mode instability are in disagreement since the boundary in the previous result by Païdoussis and Issid (1974) is not straight (See Figs. 9 and 10(b) in their paper). To determine the boundaries numerically, numerical simulations were carried out by solving Eq. (7) directly in the neighborhood of these boundaries. When $\alpha \neq 0$, it is easy to determine the boundaries with the numerical method since at the points out of the unstable regions the responses to all initial disturbances always decay with passage of time. In Fig. 4(c), the instability boundary for $M_r = 0.8$ in Fig. 4(a) is plotted applying our analytical method with varying α. The instability boundaries for $\alpha \neq 0$ in Fig. 4(c) can also be determined with the numerical method mentioned above, and the boundaries of the theoretical result were found to be in good agreement with that of the numerical result. It is easy to see from the figure that the straight boundary for $\alpha = 0$ in the present result is the natural limit of the boundary lines when $\alpha \to 0$. However, the boundaries for $\alpha = 0$ cannot be determined with the numerical method directly, because in this case the response to any initial disturbance no longer decays with passage of time (the system becomes a conservative system when $\alpha = 0$).

5. Parametric resonances

We now consider the nonlinear behavior of pipes when parametric resonances occur. In Appendix A, the nonlinear term $\mathbf{f}(\mathbf{x})$ in Eq. (11) was neglected in deriving the stability regions of the trivial solution. Now, retaining the nonlinear

term neglected and doing the same procedure of averaging as done in Appendix A for Eq. (11), one can obtain the equation of the response curves, which gives the relation between the amplitude and frequency for the steady state responses, by setting $\dot{a}_i = 0$ and $\dot{\theta}_i = 0$ (for $i = 1, 2$) in the resulting averaged equations. This procedure and calculation are quite laborious, and so we do not attempt to give the explicit analytical formulation of the equation here. We give only some numerical results of the response curves for some given parameter values, according to this equation. In Figs. 5(a) and (b) the various response curves (obtained by varying μ) are given in the $\omega - a$ plane, where a represents the amplitudes of the first and second mode resonances, for the parametric resonances of the first and second modes[1]. The same responses in Figs. 5(a) and 5(b) are plotted in the $\omega - \eta_a$ plane in Figs. 5(c) and (d), where, and in what follows, η_a represents the dimensionless amplitude of the pipe at a point, say $\xi = 0.65$. The upper portion of the response curves indicated by the solid lines in Fig. 5 corresponds to the stable periodic motions (the parametric resonances of the pipe), and the lower portion of the response curves represented by the dotted lines corresponds to the unstable periodic motions. We explain such a nonlinear response of the system through an example for the first mode resonance of the pinned-pinned pipe for $\mu = 0.4$ (see Figs. 5(a) and (c)). In the region of $\omega < \mathrm{A}$ in Figs. 5(a) and (c) the trivial solution, which corresponds to the undeformed state of the pipe, is stable, and the responses to all initial disturbances decay with passage of time. In region of $\mathrm{A} < \omega < \mathrm{B}$, the trivial solution is unstable, and any initial disturbance can produce a steady state periodic response (i.e., the sub-harmonic resonance with the first mode). If the initial amplitude is very large, the response will decay until steady state motion is reached. On the other hand, if the initial disturbance is very small, the response will grow to reach the condition of steady-state motion. Thus in region of $\mathrm{A} < \omega < \mathrm{B}$, all initial disturbances, regardless of how large or how small the amplitude, always produce the same steady-state periodic motion for a given value of ω, that is, a limit cycle motion exists. In region of $\omega > \mathrm{B}$, the response to an initial disturbance may either decay to the trivial solution or achieve a sustained periodic motion (a limit cycle corresponding to the sub-harmonic resonance with the first mode). The boundary separating the two domains of attraction in the state space is the unstable periodic motion (unstable limit cycle) corresponding to motions indicated by the dotted lines in Figs. 5(a) and (c).

It is noted that the above results of nonlinear response shown in Fig. 5, and similar results given in the investigations by Namachchivaya (1989) and Namachchivaya and Tien (1989a, b), are obtained from the equation of averaging. As indicated previously in the Introduction, since the detuning of frequency, λ, is a small parameter used in the method of averaging, the amplitude–frequency relationship given in these results is valid only in the vicinity of the resonances. Therefore, the analysis for the nonlinear responses in terms of the averaged nonlinear equation is meaningless for the case when the exciting frequency goes far away from the resonance region. Comparison of nonlinear responses between the results of averaged equation and the results obtained by solving directly the original equation (7) numerically is made in Figs. 5(c) and (d) for $\mu = 0.4$ for a pinned–pinned pipe and for $\mu = 0.25$ for a clamped-clamped pipe, respectively. Regarding the numerical results in Figs. 5(c) and (d), we will give a more detailed explanation in the next two subsections.

Some numerical methods for solving the equation of motion are applied in the next subsections to investigate the dynamical behavior of the system. Especially, we are interested to investigate how far the regions of parametric vibrations can extend away from the resonance regions and what would occur in the regions far away from the resonance regions. The amplitude–frequency response curves and their properties are studied for some given parameter values through tracing the response curves numerically from the region of resonance to that of non resonance. We give two numerical examples in Sections 5.1 and 5.2:

$$u_0 = 1.88, \quad M_r = 0.8, \quad \alpha = 0.005, \quad \gamma = 5000, \quad \overline{g} = T = 0, \quad \mu = 0.4 \tag{22}$$

for the pinned–pinned pipe; and

$$u_0 = 4.0, \quad M_r = 0.447, \quad \alpha = 0.001, \quad \gamma = 5000, \quad \overline{g} = T = 0, \quad \mu = 0.25 \tag{23}$$

for the clamped–clamped pipe, to discuss the properties of nonlinear response obtained via these numerical studies.

5.1. Parametric resonances of pinned–pinned pipe

Corresponding to the parameter values given in Eqs. (22), the undamped natural frequencies of the first and second modes of the system are $\omega_1 = 7.716$ and $\omega_2 = 38.602$, respectively. The stability regions and the amplitude–frequency

[1]In the papers by Namachchivaya (1989) and Namachchivaya and Tien (1989a,b) the value of the coefficient of the nonlinear term k (which corresponds to the coefficient of nonlinear term γ in the present paper) in the equation of motion was not given in their numerical examples, and so the nonlinear responses shown in Fig. 5 could not be compared with their results.

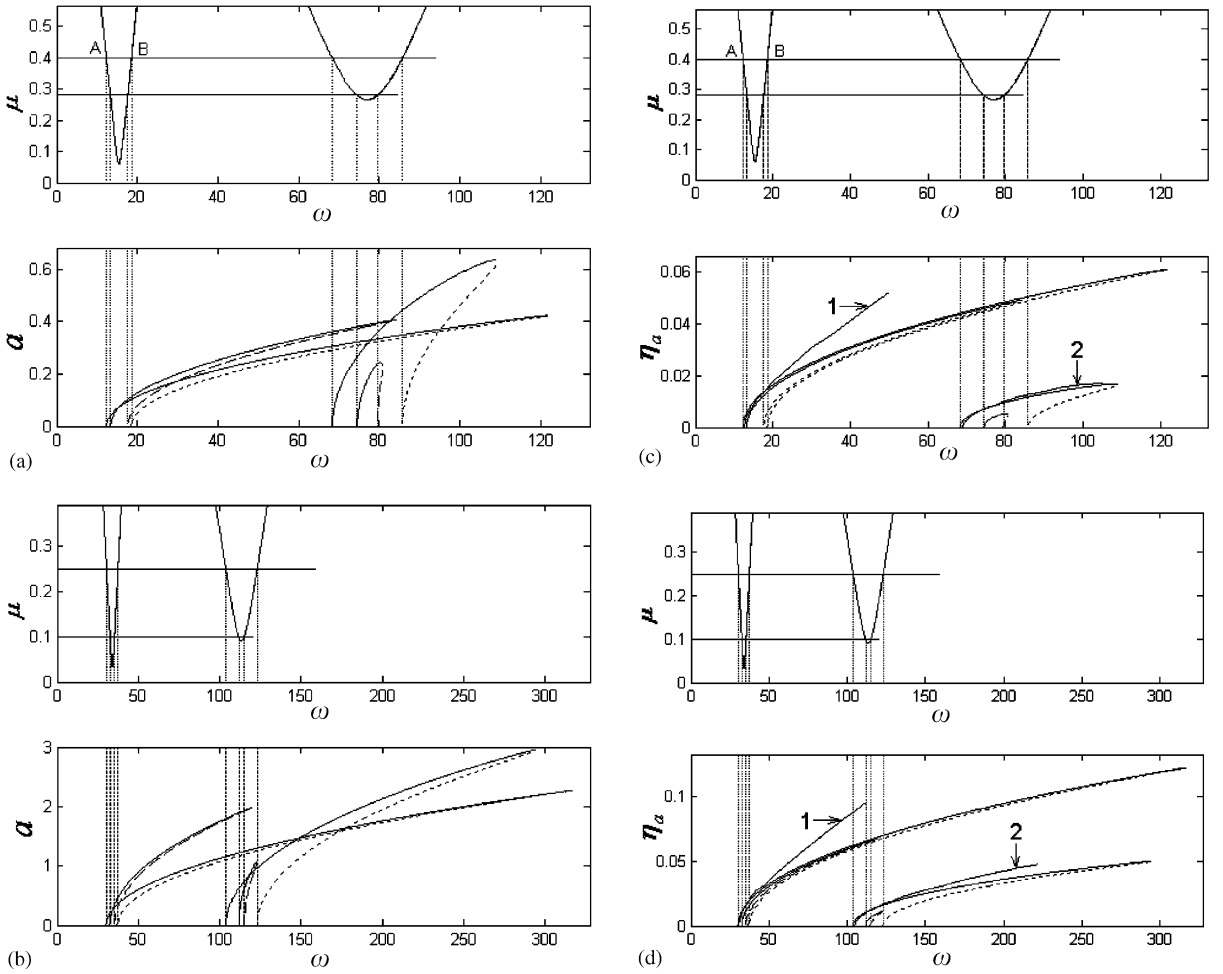

Fig. 5. Nonlinear response curves of parametric resonances with the first and second modes. (a) The response curves in the $\omega - a$ plane for a pinned-pinned pipe with $\mu = 0.28$ and 0.4 ($u_0 = 1.88$, $M_r = 0.8$, $\alpha = 0.005$, $\gamma = 5000$, $\overline{g} = T = 0$). (b) The response curves in the $\omega - a$ plane for a clamped- clamped pipe with $\mu = 0.1$ and 0.25 ($u_0 = 4.0$, $M_r = 0.447$, , $\alpha = 0.001$, $\gamma = 5000, \overline{g} = T = 0$). (c) The response curves in $\omega - \eta_a$ plane for the same system as in (a). In the figure, 1 and 2 represents the response curves of the first and second modes, respectively, obtained with numerical method for $\mu = 0.4$. (d) The response curves in $\omega - \eta_a$ plane for the same system as in (b). In the figure, 1 and 2 represent the response curves of the first and second modes, respectively, obtained with numerical method for $\mu = 0.25$.

response curves are shown in Figs. 6(a) and 6(b), respectively. The response curves in the figure are obtained through tracing the resonance responses by solving Eq. (7) numerically with increasing frequency ω incrementally.

5.1.1. *Simple parametric resonances*

We now analyze numerically two simple parametric resonances: the sub-harmonic resonances of order $\frac{1}{2}$ for the first and second modes. The frequencies corresponding to the boundary points A and B (see Fig. 6(a)) in the resonance region of the first mode for $\mu = 0.4$ are $\omega_A \approx 12.7$ and $\omega_B = 19.6$, respectively, which are located to the left and right of $\omega_0 = 2\omega_1 = 15.432$, respectively. As ω is increased from the left of ω_A, the pipe loses stability at $\omega = \omega_A$, and a sub-harmonic resonance of the first mode takes place. In fact, the trivial solution of the associated averaged system loses stability at $\omega = \omega_A$ through a simple bifurcation (the linear part of the system has a zero eigenvalue at that point) (Namachchivaya, 1989). The amplitude of the resonance is increased with increasing ω, and we have tracked the motions up to $\omega = 51.3$ (see Fig. 6(b)). An example of such a sub-harmonic resonance with the first mode for $\omega = 46$ is shown in Fig. 7(a). In this figure, and in what follows, the axes η and $\dot{\eta}$ represent the nondimensional displacement and

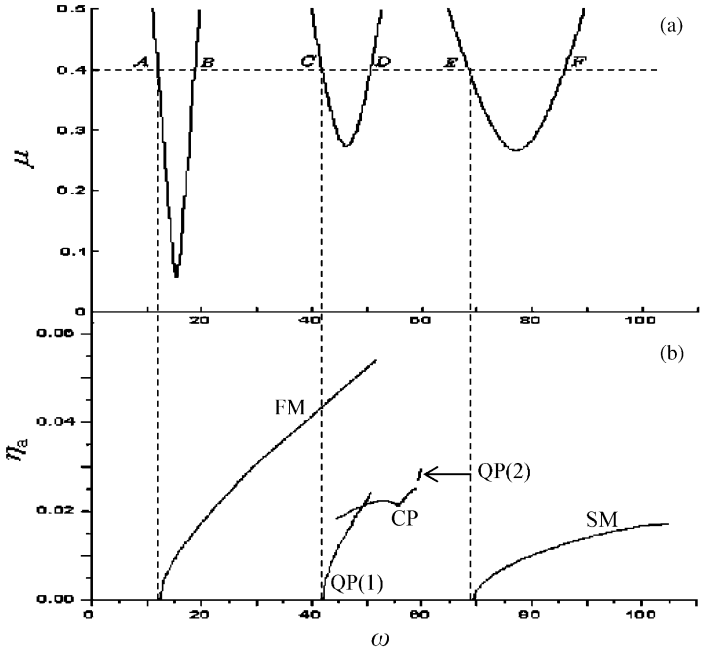

Fig. 6. (a) Stability boundaries for pinned–pinned pipe. (b) Amplitude–frequency response curves for $\mu = 0.4$. FM: first mode subharmonic resonance; SM: second mode sub-harmonic resonance; QP: quasiperiodic motion; CP: combined periodic motion.

velocity of the pipe at $\xi = 0.65$. As seen from Fig. 7(a) the resonance is nearly a simple harmonic motion with the basic frequency $\omega_f = 23.022$, which is related to the exciting frequency ω by $2\omega_f \approx \omega$.

The frequencies corresponding to the boundary points E and F (see Fig. 6(a)) in the resonance region of the second mode for $\mu = 0.4$ are $\omega_E \approx 69.7$ and $\omega_F = 87$, respectively, which are located to the left and right of $\omega_0 = 2\omega_2 = 77.204$, respectively. As ω is increased from the left of ω_E, the pipe loses stability at $\omega = \omega_E$, and the subharmonic resonance of the second mode occurs. The amplitude of the resonance is increased with increasing ω, and we have tracked the motions numerically up to $\omega = 105$. An example of such a motion for $\omega = 77$ is shown in Fig. 7(b). Like the resonance of the first mode, the motion is also nearly simple harmonic with a basic frequency $\omega_s = 38.371$, related to ω by $2\omega_s \approx \omega$. The relationship between the basic frequencies of sub-harmonic motions and the frequency of excitation is shown in Fig. 8.

5.1.2. *Combination parametric resonances*

The frequencies corresponding to the boundary points C and D (see Fig. 6(a)) in the region of the combination resonance for $\mu = 0.4$ are $\omega_C \approx 42.6$ and $\omega_D \approx 50.1$, respectively, which are located to the left and right of $\omega_0 = \omega_1 + \omega_2 = 46.318$. It is shown that, as ω is increased from the left of ω_C, the trivial solution in the corresponding averaged system loses stability by a Hopf bifurcation at $\omega = \omega_C$ (Namachchivaya and Tien, 1989a); therefore, in the original system the pipe loses stability also at $\omega = \omega_C$, and a quasiperiodic motion takes place. We tracked numerically such motions up to $\omega = 50.8$. The numerical simulations of such a quasiperiodic motion for $\omega = 46$ are shown in Figs. 7(c)–(e). It may be seen from Fig. 7(e) that the motion has two basic frequencies of $\omega_{q1} \approx 9.738$ ($f_{q1} \approx 1.557$) and $\omega_{q2} \approx 36.257$ ($f_{q2} \approx 5.771$). For a quasiperiodic motion, these two basic frequencies should be incommensurate (Nayfeh and Balachandran, 1995), and the Poincaré maps of response form a closed loop (Fig. 7(d)). The relationship between the basic frequencies of the combination resonance, denoted by "quasiperiodic (1)", and the exciting frequency is shown in Fig. 9. It is easy to see from the figure that there always exists the relation of $\omega \approx \omega_{q1} + \omega_{q2}$, that is, the sum of the two basic frequency values of the combination resonance is approximately equal to the value of the exciting frequency ω.

In addition to the quasiperiodic motions mentioned above, we found some periodic motion in the region of the combination resonance, and it will be called *combined periodic motion* in what follows. The region where the periodic motions exist is $\omega \approx 44.9-59.3$. An example of such a combined periodic motion at $\omega = 46$ is shown in Figs. 7(f) and

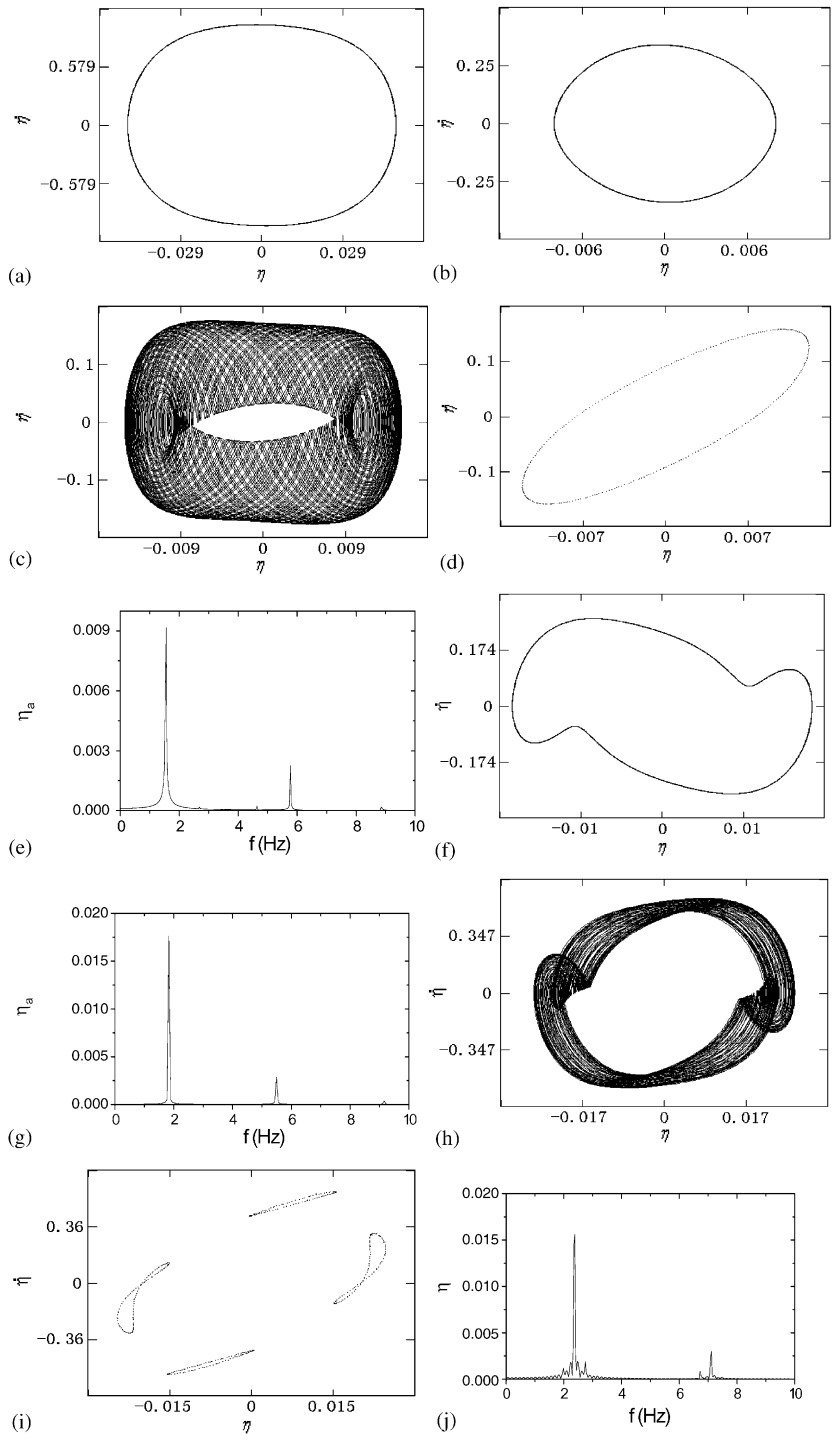

Fig. 7. Numerical simulations for pinned–pinned pipe. (a) Sub-harmonic resonance with the first mode for $\omega = 46$. (b) Sub-harmonic resonance with the second mode for $\omega = 77$. (c) Quasiperiodic motion for $\omega = 46$. (d) Poincaré Map of the motion in (c). (e) Amplitude spectrum of the motion in (c). (f) Combined periodic motion for $\omega = 46$. (g) Amplitude spectrum of the motion in (f). (h) Quasiperiodic motion for $\omega = 59.5$. (i) Poincaré Map of the motion in (h). (j) Amplitude spectrum of the motion in (h).

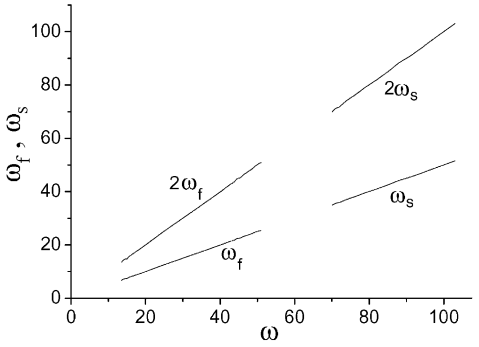

Fig. 8. Relationship between the basic frequencies (ω_f and ω_s) of sub-harmonic motions with the first and second modes and the frequency (ω) of excitation, for pinned-pinned pipe.

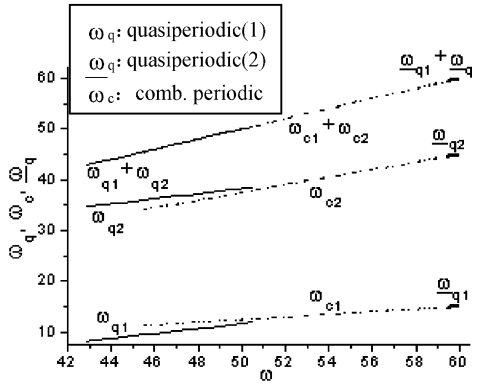

Fig. 9. Relationship between the basic frequencies of the quasiperiodic motion(1) (ω_{qi}), combined periodic motion (ω_{ci}) and quasiperiodic motion(2) ($\underline{\omega}_{qi}$) and the frequency (ω) of excitation, for pinned–pinned pipe.

(g). It is seen from the figures that the motion also has two basic frequencies of $\omega_{c1} = 11.511$ ($f_{c1} = 1.832$) and $\omega_{c2} = 34.534$ ($f_{c2} = 5.496$) , which are related to the exciting frequency ω by $\omega \approx \omega_{c1} + \omega_{c2}$. Since the motion is periodic, the basic frequencies ω_{c1} and ω_{c2} should be commensurate (Nayfeh and Balachandran, 1995). The relationship between the basic frequencies of the combined periodic motions and the exciting frequency is also shown in Fig. 9. It is not known yet whether the combined periodic motion is born at $\omega = \omega_C$ together with the quasiperiodic motions, since this motion has not been captured near the Hopf bifurcation point in our numerical analysis. Note that as ω is increased further, a change in the motion takes place near $\omega \approx 59.4$ from the combined periodic motion, and another type of quasiperiodic motion (which differs from the previous one) appears in the region of $\omega = 59.4-59.95$. An example of such a quasiperiodic motion for $\omega = 59.5$ is shown in Figs. 7(h)–(j). The relationship between the basic frequencies of the quasiperiodic motions, which are denoted by "quasiperiodic(2)", and the exciting frequency is also shown in Fig. 9.

It is noted in Fig. 6(b) that the sub-harmonic resonance curve of the first mode extends as far as the region of the combination resonance. This phenomenon may lead to multiple responses of steady state oscillation at the same exciting frequency ω in the overlap regions of different resonance curves, as shown in Table 1. In region 1 ($\omega \approx 42.6-44.6$) two different motions, the sub-harmonic response of the first mode and the quasiperiodic motion, can arise corresponding to every value of ω in the region, and similarly, three and two different motions can occur in region 2 ($\omega \approx 44.7-50.8$) and region 3 ($\omega \approx 50.9-51.3$), respectively.

It should be noticed that in the previous numerical examples for the sub-harmonic motion of the first mode in Fig. 7(a), quasiperiodic motion in Fig. 7(c) and combined periodic motion in Fig. 7(f), the exciting frequency ω is always taken to be $\omega = 46$, which lies in region 2 in Table 1. The condition that makes the system to have different behavior at the same exciting frequency ($\omega = 46$) is just the different initial values associated with each motion. Every motion in such regions where the system has multiple responses at the same frequency ω possesses its domain of attraction in the

Table 1
The regions of multiple responses, for pinned–pinned pipe

Number of region	1	2	3
Range of frequency, ω	42.6–44.6	44.7–50.8	50.9–51.3
Possible motions	①,②	①,②,③	①,③

① Sub-harmonic motion of first mode; ② quasiperiodic motion(1); ③ combined periodic motion.

state space. If the motion of the system in such a region is subjected to a shock which is large enough, then a sudden change of motion from one steady state to another probably takes place in some cases. Such a phenomenon (the sudden change of motion) is different from the jump phenomenon in amplitude, which may be seen in standard books on nonlinear forced oscillations. The change of motion in the latter case manifests itself in the magnitude of amplitude, while in the former case it involves not only the amplitude but the type of motion and the frequency relation between the response and excitation. It should also be noted that in the previous numerical examples of Fig. 7(a), (c) and (f) there is a certain relation between the three different responses and the excitation, that is,

$$2\omega_f \approx \omega_{q1} + \omega_{q2} \approx \omega_{c1} + \omega_{c2} \approx \omega = 46.$$

Similar relations can be found in each region in Table 1.

$$\begin{aligned}&\text{Region 1}: \ 2\omega_f \approx \omega_{q1} + \omega_{q2} \approx \omega;\\ &\text{Region 2}: \ 2\omega_f \approx \omega_{q1} + \omega_{q2} \approx \omega_{c1} + \omega_{c2} \approx \omega;\\ &\text{Region 3}: \ 2\omega_f \approx \omega_{c1} + \omega_{c2} \approx \omega.\end{aligned} \tag{24}$$

5.2. Parametric resonances of clamped-clamped pipe

We now analyze some properties of the parametric resonances for a clamped–clamped pipe, applying the same numerical method as used in the previous subsection for the pinned–pinned pipe. Some fixed parameter values used are given in Eq. (23). The natural frequencies of the first and second modes of the system corresponding to these parameter values are $\omega_1 = 16.996$ and $\omega_2 = 56.784$, respectively. The stability regions and the (stable) amplitude-frequency response curves are shown in Figs. 10(a) and (b), respectively.

5.2.1. Simple parametric resonances

The simple parametric resonances of the first and second modes are investigated numerically in this subsection for a clamped–clamped pipe, in the same way as was done in Section 5.1.1 for the pinned-pinned pipe.

The frequencies corresponding to the boundary points A and B (see Fig. 10(a)) in the region of the first mode sub-harmonic resonance for $\mu = 0.25$ are $\omega_A \approx 30.5$ and $\omega_B \approx 37.4$, respectively, which are located to the left and the right of $\omega_0 = 2\,\omega_1 = 33.992$, respectively. As ω is increased from the left of ω_A the pipe loses stability at $\omega = \omega_A$, and then the subharmonic resonance of the first mode arises. The amplitude of the resonance is increased with increase of ω, and we tracked the motions numerically up to $\omega = 116$ (see Fig. 10(b)). The resonance is a nearly simple harmonic motion, like the case of pinned-pinned pipe shown in Fig. 7(a), and the frequencies of the response and excitation are related by $2\omega_f \approx \omega$.

The frequencies corresponding to the boundary points E and F (see Fig. 10(a)) in the resonance region of the second mode for $\mu = 0.25$ are $\omega_E \approx 104.8$ and $\omega_F \approx 123.8$, respectively, which are located to the left and the right of $\omega_0 = 2\,\omega_2 = 113.568$, respectively. As ω is increased from the left of ω_E the pipe loses stability at $\omega = \omega_E$, and then the sub-harmonic resonance of the second mode takes place. The amplitude of the resonance is increased with increasing ω, and we tracked such motions numerically up to $\omega = 225$. The motion is also nearly simple harmonic, and the basic frequency ω_s is related to the exciting frequency ω by $2\omega_s \approx \omega$.

5.2.2. Combination parametric resonances

The frequencies corresponding to the points C and D (see Fig. 10(a)) in the boundary of the combination resonance region for $\mu = 0.25$ are $\omega_C \approx 70.9$ and $\omega_D \approx 76.1$, respectively, which are located to the left and the right of $\omega_0 = \omega_1 + \omega_2 = 73.78$, respectively. As ω is increased from the left of ω_C the trivial solution in the averaged system

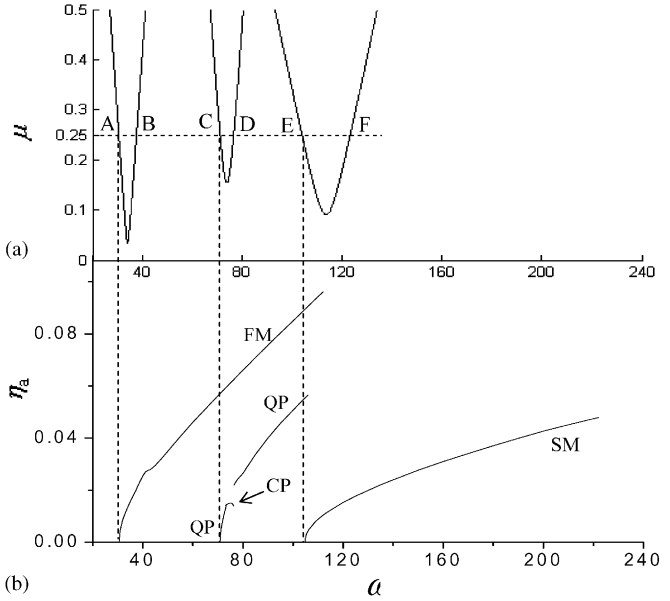

Fig. 10. (a) Stability boundaries for clamped–clamped pipe. (b) Amplitude–frequency response curves for $\mu = 0.25$. FM: first-mode sub-harmonic resonance; SM: second-mode sub-harmonic resonance; QP: quasiperiodic motion; CP: combined periodic motion.

Table 2
The regions of multiple responses, for clamped–clamped pipe

Number of region	1	2	3	4	5	6
Range of frequency, ω	70.9–73	73.1–73.4	73.5–76.3	76.4–104.7	104.8–109	109.1–116
Possible motions	①,③	①,③,④	①,④	①,③	①,②,③	①,②

① Sub-harmonic motion of first mode; ② sub-harmonic motion of second mode; ③ quasiperiodic motion; ④ combined periodic motion.

loses stability by the Hopf bifurcation at $\omega = \omega_C$, and hence a quasiperiodic motion arises in the original system. The frequency ranges of the quasiperiodic motions found in the numerical investigation are $\omega \approx 70.9-73.4$ and 76.4–109. The motion has two basic frequencies of ω_{q1} and ω_{q2}, and they always satisfy the relationship $\omega \approx \omega_{q1} + \omega_{q2}$. As indicated in the previous subsection, these two frequencies should be incommensurate. Like the case of pinned-pinned pipe, in the region of the combination resonance some periodic motion (called combined periodic motion) exists in addition to the quasiperiodic motions mentioned above. The region where the periodic motions exist is $\omega \approx 73.1-76.3$. The motion has two basic frequencies of ω_{c1} and ω_{c2}, which are related to the exciting frequency ω by $\omega \approx \omega_{c1} + \omega_{c2}$.

It is noted that the combination resonance curve in Fig. 10(b) extends as far as the region of the sub-harmonic resonance of the second mode, and the first mode resonance curve covers completely the whole region of the combination resonance and extends as far as the region of the second mode resonance. As indicated in the previous subsection for the case of a pinned–pinned pipe, the multiple responses of steady-state oscillation will occur in these overlap regions of different resonance curves, as shown in Table 2. There are certain relations between the different responses and the excitation in each region in Table 2, as follows:

$$\text{Region 1}: \ 2\omega_f \approx \omega_{q1} + \omega_{q2} \approx \omega;$$
$$\text{Region 2}: \ 2\omega_f \approx \omega_{q1} + \omega_{q2} \approx \omega_{c1} + \omega_{c2} \approx \omega;$$
$$\text{Region 3}: \ 2\omega_f \approx \omega_{c1} + \omega_{c2} \approx \omega;$$

$$\begin{aligned}&\text{Region 4}: \ 2\omega_f \approx \omega_{q1} + \omega_{q2} \approx \omega;\\ &\text{Region 5}: \ 2\omega_f \approx \omega_{q1} + \omega_{q2} \approx 2\omega_s \approx \omega;\\ &\text{Region 6}: \ 2\omega_f \approx 2\omega_s \approx \omega.\end{aligned} \tag{25}$$

5.3. Summary

In general, the nonlinear equation of motion of a physical system, such as Eq. (11), has many solutions other than those that are periodic, and so it is difficult to give a general analytical method for determining the nonlinear behavior of the system in a global region. This allows us to think naturally of using numerical methods to determine the nonlinear behavior of the system when parametric resonances occur. Numerical computations that we have carried out for various parameter values shows that a similar qualitative behavior of the nonlinear responses as those shown in Sections 5.1 and 5.2 can be obtained when the parameters take different values than those given by Eqs. (22) and (23). This behavior may be summarized as follows.

(a) The overlap regions of the different parametric resonances always exist, though the ranges of the regions are somewhat different according to the different parameter values. This implies that there is always the possibility that several different parametric resonances take place in the system, corresponding to the same value of the exciting frequency ω in certain circumstances.

(b) If the multiple responses mentioned in (a) take place, then there is always a certain relation of frequencies between the different responses and the excitation, such as Eqs. (24) and (25) in the examples given in Sections 5.1 and 5.2. This is an interesting phenomenon from the physical point of view. To explain this we need a careful analytical study of the structure of the solution of Eq. (11) in a global sense, though this is very difficult for a nonlinear equation.

(c) In the region of combination resonance, we always find quasiperiodic motions and combined periodic motions, even though the configurations of these response curves change somewhat according to the different parameter values. In addition, the results of numerical calculations show that the combined periodic motions seem to possess the character of $f_{c2} \approx 3f_{c1}$, always. In Tables 3 and 4, the numerical results for some sample points of ω for the combined periodic motions are shown for pinned–pinned and clamped–clamped pipes, respectively. It is easy to see the relations of $f_{c1} + f_{c2} \approx f$ and $f_{c2} \approx 3f_{c1}$ from the tables. In a subsequent paper, the authors hope to provide a discussion on this issue together with an analytical method. We know that the response curve of quasiperiodic motion is initiated from the point where the Hopf bifurcation occurs in the corresponding averaged equation, whereas for the combined periodic motion, it is not yet known exactly where the beginning of the response curve is.

Table 3
Combined periodic motions, for pinned–pinned pipe

ω	46	47	49	51	53	55	57	58
$f\left(=\frac{\omega}{2\pi}\right)$	7.32113	7.48028	7.7986	8.1169	8.43521	8.75352	9.07183	9.23099
f_1	1.78659	1.89313	1.9542	2.0429	2.1304	2.19189	2.28148	2.31167
f_2	5.35976	5.61832	5.89313	6.1287	6.36077	6.6061	6.82922	6.93502
$3f_1$	5.35977	5.67939	5.8626	6.1287	6.3912	6.57567	6.84444	6.93501
f_1+f_2	7.14635	7.51145	7.84733	8.1716	8.49117	8.79799	9.1107	9.24669

Table 4
Combined periodic motions, for clamped–clamped pipe

ω	73	74	75	76
$f\left(=\frac{\omega}{2\pi}\right)$	11.61831	11.77747	11.93662	12.09578
f_1	2.9313	2.94823	2.99237	3.0229
f_2	8.73282	8.8244	8.94656	9.0687
$3f_1$	8.7939	8.84469	8.97711	9.0687
f_1+f_2	11.66412	11.77263	11.93893	12.0916

6. Conclusions

In this paper, the parametric resonances of pipes with supported ends conveying pulsating fluid have been analyzed by means of numerical methods. According to the stability criterion derived, the effect of some physical parameters of the system, such as damping, mean flow velocity, mass ratio, tension and gravity, on the three regions of parametric resonances has been discussed. The amplitude–frequency response curves of parametric resonances and their frequency characteristics have been investigated through numerical simulations. The results obtained show that several motions may arise in the region of combination resonance, including quasiperiodic and combined periodic motions.

There exist some regions of overlap between the regions of the different resonances, and hence the multiple responses of steady state oscillation may occur at the same value of the exciting frequency ω in these overlap regions. This phenomenon may lead to sudden changes in motion from one steady state response to another in some cases. The change can occur not only in the amplitude of oscillation, but in the type of motion and in the frequency relation between the response and the excitation. If multiple responses take place, then there is always a certain frequency relationship between the different responses and the excitation.

Acknowledgement

This research was supported by the National Natural Science Foundation of China under Project No: 10372063. The authors would like to thank Dr X. D. Yang and Mr J. L. Zhang for their assistance in the numerical calculations.

Appendix A

Expressions (14), (16) and (18), via which the boundaries of the resonance regions are determined, can be derived by using the method of averaging. In deriving these expressions in a previous study by Ariaratnam and Namachchivaya (1986) some advanced analysis was used, such as the symplectic transformation method of Hamiltonian systems. We now wish to give the essence of the procedure for deriving these expressions with a more regular process and, in addition, to consider further the effect of some parameters that were not considered in previous study.

Substituting Eq. (13) into Eq. (11), we obtain

$$\dot{\mathbf{x}} = \hat{\mathbf{\Omega}}\mathbf{x} + \mu(-\bar{\lambda}\hat{\mathbf{\Omega}}\mathbf{x} + \mathbf{G} - \mathbf{f}(\mathbf{x})/\omega_0), \tag{A.1}$$

where

$$\hat{\mathbf{\Omega}} = \frac{\mathbf{\Omega}}{\omega_0} = \begin{pmatrix} \mathbf{K_1} & \mathbf{O} \\ \mathbf{O} & \mathbf{K_2} \end{pmatrix}, \quad \mathbf{K}_i = k_i \begin{pmatrix} 0 & -1 \\ 1 & 0 \end{pmatrix} (i = 1, 2), \quad \mathbf{O} = \begin{pmatrix} 0 & 0 \\ 0 & 0 \end{pmatrix}, \quad k_1 = \frac{\omega_1}{\omega_0}, \quad k_2 = \frac{\omega_2}{\omega_0},$$

$$\mathbf{G} = (g_{11}, g_{12}, g_{21}, g_{22})^{\mathrm{T}} \equiv (\mathbf{A}_1 \sin\tau - (\mathbf{A}_2 \cos\tau)/\omega_0 - \bar{\alpha}\mathbf{A}_3/\omega_0)\mathbf{x}. \tag{A.2}$$

In deriving Eq. (A.1) we used the fact that

$$\frac{1}{1 + \mu\bar{\lambda}} = 1 - \mu\bar{\lambda} + \mathcal{O}(\mu^2).$$

In this paper, only the cases of $\omega_0 = 2\omega_1$ (or $k_1 = 1/2$), $\omega_0 = 2\omega_2$ (or $k_2 = 1/2$) and $\omega_0 = |\omega_1 \pm \omega_2|$ (or $1 = |k_1 \pm k_2|$) are considered.

In order to transform Eq. (A.1) into equations of the amplitude-phase form, we introduce the following transformations:

$$x_{2i-1} = a_i \cos\varphi_i, \quad x_{2i} = a_i \sin\varphi_i, \quad (i = 1, 2), \tag{A.3}$$

where

$$\varphi_1 = k_1\tau + \theta_1, \quad \varphi_2 = k_2\tau + \theta_2, \tag{A.4}$$

a_1, a_2, θ_1 and θ_2 being functions of τ. The nonlinear term, **f(x)**, in Eq. (A.1) need not be considered for the stability analysis of the trivial solution, i.e., the undeformed state of the pipes, except for some of the degenerate cases.

Letting $\mathbf{f}(\mathbf{x}) = 0$ in Eq. (A.1) and substituting Eq. (A.3) and (A.4) into Eq. (A.1) and solving it for $\dot{a}_i$ and $a_i\dot{\theta}_i$, we obtain

$$\dot{a}_i = \mu[(\bar{\lambda}k_i a_i \sin\varphi_i + g_{i1})\cos\varphi_i + (-\bar{\lambda}k_i a_i \cos\varphi_i + g_{i2})\sin\varphi_i],$$

$$a_i\dot{\theta}_i = \mu[(-\bar{\lambda}k_i a_i \cos\varphi_i + g_{i2})\cos\varphi_i - (\bar{\lambda}k_i a_i \sin\varphi_i + g_{i1})\sin\varphi_i] \quad (i=1,2), \tag{A.5}$$

where g_{ij} is defined in Eq. (A.2).

Applying the averaging operator, $\lim_{T\to\infty}(1/T)\int_0^T(\,)\,\mathrm{d}\tau$, to Eq. (A.5) one obtains a set of averaged equations

$$\begin{aligned}\dot{a}_i &= \lim_{T\to\infty}\tfrac{1}{T}\int_0^T \mu(g_{i1}\cos\varphi_i + g_{i2}\sin\varphi_i)\,\mathrm{d}\tau,\\ a_i\dot{\theta}_i &= -\lambda k_i a_i + \lim_{T\to\infty}\tfrac{1}{T}\int_0^T \mu(g_{i2}\cos\varphi_i + g_{i1}\sin\varphi_i)\,\mathrm{d}\tau,\end{aligned} \quad (i=1,2). \tag{A.6}$$

In the above equations, no distinction has been made between the averaged and nonaveraged variables for notational convenience. We shall now discuss a number of special cases that arise from the special choices of the parameters k_1 and k_2.

A.1. Case of $k_1 = 1/2$ (i.e., $\tau = 2\varphi_1 - 2\theta_1$)

Let

$$2\theta_{10} = \tan^{-1}(V_1/U_1). \tag{A.7}$$

Using Eqs. (15) and (A.7), Eq. (A.6) can be written as

$$\begin{aligned}\dot{a}_1 &= (\mu/4)(U_1^2+V_1^2)^{1/2}a_1\sin(2\theta_1+2\theta_{10}) - \alpha(A_3^{11}+A_3^{22})a_1/(2\omega_0),\\ \dot{\theta}_1 &= (\mu/4)(U_1^2+V_1^2)^{1/2}\cos(2\theta_1+2\theta_{10}) - \alpha(A_3^{21}-A_3^{12})/(2\omega_0) - \lambda/2,\\ \dot{a}_2 &= -\alpha(A_3^{33}+A_3^{44})a_2/(2\omega_0),\\ \dot{\theta}_2 &= -\lambda k_2 - \alpha(A_3^{43}-A_3^{34})/(2\omega_0).\end{aligned} \tag{A.8}$$

It is noted that the motions of the first and second modes in Eqs. (A.8) are uncoupled. Numerical analysis shows that for $u_0 < u_c$, $A_3^{33}+A_3^{44}$, is always positive, and hence from the third of Eqs. (A.8) it is easy to see that the motion of the second mode will be damped out quickly. Therefore, the stability of the pipes depends ultimately on the stability of the trivial solution of the first two of Eqs. (A.8), the first mode motion.

Introducing the transformation

$$\xi_1 = a_1\cos(\theta_1+\theta_{10}), \quad \zeta_1 = a_1\sin(\theta_1+\theta_{10}) \tag{A.9}$$

and substituting it into the first two of Eqs. (A.8), we obtain

$$\begin{aligned}\dot{\xi}_1 &= \left\{(\mu/4)\left(U_1^2+V_1^2\right)^{1/2} + \left[\alpha\left(A_3^{21}-A_3^{12}\right)/(2\omega_0)+\lambda/2\right]\right\}\zeta_1 - \alpha\left(A_3^{11}+A_3^{22}\right)\xi_1/(2\omega_0),\\ \dot{\zeta}_1 &= \left\{(\mu/4)\left(U_1^2+V_1^2\right)^{1/2} - \left[\alpha\left(A_3^{21}-A_3^{12}\right)/(2\omega_0)+\lambda/2\right]\right\}\xi_1 - \alpha\left(A_3^{11}+A_3^{22}\right)\zeta_1/(2\omega_0).\end{aligned} \tag{A.10}$$

The characteristic equation of the coefficient matrix on the right side in Eqs. (A.10) may be written as

$$\rho^2 + \frac{\alpha}{2\omega_1}\left(A_3^{11}+A_3^{22}\right)\rho + \left\{\left[\frac{\alpha}{4\omega_1}\left(A_3^{11}+A_3^{22}\right)\right]^2 + \left[\frac{\alpha}{4\omega_1}\left(A_3^{21}-A_3^{12}\right)+\frac{\omega-2\omega_1}{4\omega_1}\right]^2 - \frac{\mu^2}{16}\left(U_1^2+V_1^2\right)\right\} = 0. \tag{A.11}$$

To obtain this equation we used the fact that

$$\mu\bar{\lambda} = \frac{\omega-\omega_0}{\omega_0}, \quad \omega_0 = 2\omega_1.$$

We can derive from Eq. (A.11) the stability condition of the trivial solution as

$$|\omega/\omega_1 - 2| > \left\{\mu^2\left(U_1^2+V_1^2\right) - \left[\alpha\left(A_3^{11}+A_3^{22}\right)/\omega_1\right]^2\right\}^{1/2}. \tag{A.12}$$

If this condition is not satisfied, then the pipe loses its stability by the first mode parametric resonances in the region given by inequality (14).

A.2. Case of $k_2 = 1/2$ (i.e.,$\tau = 2\varphi_2 - 2\theta_2$)

Let

$$2\theta_{20} = \tan^{-1}(V_2/U_2). \tag{A.13}$$

Substituting Eqs. (17) and (A.13) into Eqs. (A.6), we obtain

$$\begin{aligned}
\dot{a}_1 &= -\alpha(A_3^{11} + A_3^{22})a_1/(2\omega_0),\\
\dot{\theta}_1 &= -\lambda k_1 - \alpha(A_3^{21} - A_3^{12})/(2\omega_0),\\
\dot{a}_2 &= (\mu/4)(U_2^2 + V_2^2)^{1/2} a_2 \sin(2\theta_2 + 2\theta_{20}) - \alpha(A_3^{33} + A_3^{44})a_2/(2\omega_0),\\
\dot{\theta}_2 &= (\mu/4)(U_2^2 + V_2^2)^{1/2} \cos(2\theta_2 + 2\theta_{20}) - \alpha(A_3^{43} - A_3^{34})/(2\omega_0) - \lambda/2.
\end{aligned} \tag{A.14}$$

As in the previous case of $k_1 = 1/2$, the motions of the two modes are uncoupled in this case also. Numerical analysis shows that for $u_0 < u_c$, $A_3^{11} + A_3^{22}$ is always positive, and so the motion of the first mode is damped out with increasing time. Therefore, the stability of the pipe depends on the stability of the trivial solution of the last two of Eqs. (A.14), the second mode motion. Through the same procedure as used in the previous case for $k_1 = 1/2$, we obtain the stability condition of the pipe

$$|\omega/\omega_2 - 2| > \left\{\mu^2\left(U_2^2 + V_2^2\right) - \left[\alpha\left(A_3^{33} + A_3^{44}\right)/\omega_2\right]^2\right\}^{1/2}. \tag{A.15}$$

If the above condition is not satisfied, then the pipe loses its stability by the second mode parametric resonances in the region given by inequality (16).

A.3. Case of $k_1 + k_2 = 1$ (i.e., $\tau = \varphi_1 + \varphi_2 - \theta_1 - \theta_2$)

In this case the averaged Eqs. (A.6) can be written by using Eqs. (19) as

$$\begin{aligned}
\dot{a}_1 &= \frac{\mu}{4}[U_{12}a_2 \sin(\theta_1 + \theta_2) + V_{12}a_2 \cos(\theta_1 + \theta_2)] - \frac{\alpha}{2\omega_0}(A_3^{11} + A_3^{22})a_1,\\
a_1\dot{\theta}_1 &= \frac{\mu}{4}[U_{12}a_2 \cos(\theta_1 + \theta_2) - V_{12}a_2 \sin(\theta_1 + \theta_2)] - \frac{\alpha}{2\omega_0}(A_3^{21} - A_3^{12})a_1 - \lambda k_1 a_1,\\
\dot{a}_2 &= \frac{\mu}{4}[U_{21}a_1 \sin(\theta_1 + \theta_2) + V_{21}a_1 \cos(\theta_1 + \theta_2)] - \frac{\alpha}{2\omega_0}(A_3^{33} + A_3^{44})a_2,\\
a_2\dot{\theta}_2 &= \frac{\mu}{4}[U_{21}a_1 \cos(\theta_1 + \theta_2) - V_{21}a_1 \sin(\theta_1 + \theta_2)] - \frac{\alpha}{2\omega_0}(A_3^{43} - A_3^{34})a_2 - \lambda k_2 a_2.
\end{aligned} \tag{A.16}$$

Using the transformation

$$Y_1 = a_1 \cos\theta_1, \quad Y_2 = a_1 \sin\theta_1, \quad Y_3 = a_2 \cos\theta_2, \quad Y_4 = a_2 \sin\theta_2, \tag{A.17}$$

Eqs. (A.16) may be written as

$$\dot{\mathbf{Y}} = \mathbf{A}\mathbf{Y}, \mathbf{Y} = (Y_1, Y_2, Y_3, Y_4)^{\mathrm{T}}, \quad \mathbf{A} = \frac{\mu}{4}\begin{bmatrix} \overline{\mathbf{A}}_1 & \mathbf{U}_{12} \\ \mathbf{U}_{21} & \overline{\mathbf{A}}_2 \end{bmatrix},$$

$$\bar{\mathbf{A}}_i = \begin{pmatrix} -2\bar{\alpha}\Lambda_i/\omega_0 & 4\bar{\lambda}k_i \\ -4\bar{\lambda}k_i & -2\bar{\alpha}\Lambda_i/\omega_0 \end{pmatrix} (i = 1, 2), \quad \mathbf{U}_{ij} = \begin{pmatrix} V_{ij} & U_{ij} \\ U_{ij} & -V_{ij} \end{pmatrix} (ij = 12, 21). \tag{A.18}$$

The eigenvalue problem of $\mathbf{A}$ yields a quartic characteristic equation of the form

$$\Omega^4 + \alpha_1\Omega^3 + \alpha_2\Omega^2 + \alpha_3\Omega + \alpha_4 = 0, \tag{A.19}$$

where

$$\begin{aligned}
\alpha_1 &= \frac{\alpha}{\omega_0}(\Lambda_1 + \Lambda_2),\\
\alpha_2 &= \lambda^2(k_1^2 + k_2^2) + \frac{\alpha^2}{4\omega_0^2}(\Lambda_1 + \Lambda_2)^2 - \left(\frac{\mu^2}{8}B - \frac{\alpha^2}{2\omega_0^2}\Lambda_1\Lambda_2\right),
\end{aligned}$$

$$\alpha_3 = \lambda^2 \frac{\alpha}{\omega_0}(\Lambda_1 k_2^2 + \Lambda_2 k_1^2) - \frac{\alpha}{\omega_0}(\Lambda_1 + \Lambda_2)\left(\frac{\mu^2}{16}B - \frac{\alpha^2}{4\omega_0^2}\Lambda_1\Lambda_2\right),$$

$$\alpha_4 = \left(\frac{\mu^2}{16}B - \frac{\alpha^2}{4\omega_0^2}\Lambda_1\Lambda_2 - \lambda^2 k_1 k_2\right)^2 + \lambda^2 \frac{\alpha^2}{4\omega_0^2}(k_1\Lambda_2 - k_2\Lambda_1)^2. \tag{A.20}$$

If we define

$$\alpha_5 \equiv \frac{4\alpha^2}{\omega_0^2}\left[\lambda^2\Lambda_1\Lambda_2 - (\Lambda_1 + \Lambda_2)^2\left(\frac{\mu^2}{16}B - \frac{\alpha^2}{4\omega_0^2}\Lambda_1\Lambda_2\right)\right]\left[\lambda^2(k_1 - k_2)^2 + \frac{\alpha^2}{4\omega_0^2}(\Lambda_1 + \Lambda_2)^2\right] \tag{A.21}$$

then, according to the Routh–Hurwitz criterion, the stability condition of the trivial solution is $\alpha_i > 0$ $(i = 1, 2, \ldots, 5)$. It is easy to see from Eqs. (A.20) and (A.21) that α_1 and α_4 are always positive, and α_2, α_3 and α_5 are all positive if

$$\frac{\mu^2}{4}B \le \frac{\alpha^2}{\omega_0^2}\Lambda_1\Lambda_2 \tag{A.22}$$

and, therefore, the trivial solution is stable in this case. If

$$\frac{\mu^2}{4}B > \frac{\alpha^2}{\omega_0^2}\Lambda_1\Lambda_2 \tag{A.23}$$

then it is easy to show that α_2,α_3 and α_5 are all positive when

$$\lambda^2\Lambda_1\Lambda_2 > (\Lambda_1 + \Lambda_2)^2\left(\frac{\mu^2}{16}B - \frac{\alpha^2}{4\omega_0^2}\Lambda_1\Lambda_2\right), \tag{A.24}$$

therefore, the trivial solution is also stable in this case. If inequality (A.24) is not satisfied, then $\alpha_5 \le 0$, and the pipe loses its stability by the combination parametric resonances in the corresponding region. The equation of the boundary curve of this region may be written as

$$\mu = 4\left\{\frac{\Lambda_1\Lambda_2}{B}\left[\left(\frac{\alpha}{2\omega_0}\right)^2 + \left(\frac{\omega - \omega_0}{\omega_0}\right)^2\left(\frac{1}{\Lambda_1 + \Lambda_2}\right)^2\right]\right\}^{1/2}. \tag{A.25}$$

A.4. Case of $k_1 - k_2 = 1$ (i.e., $\tau = \varphi_2 - \varphi_1 + \theta_1 - \theta_2$)

It can be shown that the pipe is always stable in this case, and hence no parametric resonances can take place.

Comparing expressions (A.12) and (A.15) with expression (27) in the paper by Ariaratnam and Namachchivaya (1986), it is easy to see that they are identical if we note the following correspondence between the notations in two papers

Present paper	Paper by Ariaratnam and Namachchivaya (1986)
ω	ν
μ, ω_r	μ, ω_r
U_r, V_r	U_{rr}, V_{rr}
Λ_1, Λ_2	ς_{11}, ς_{22}
U_{12}, U_{21}, V_{12}, V_{21}	U_{12}, U_{21}, V_{12}, V_{21}
B	$U_{12}U_{21} + V_{12}V_{21}$

We see also that inequality (A.24) above and inequality (37) in the paper by Ariaratnam and Namachchivaya (1986) are, in fact, equivalent. If both sides in the latter expression are squared, we can easily derive from the resulting expression the identical inequality as (A.24).

References

Ariaratnam, S.T., Namachchivaya, N.S., 1986. Dynamic stability of pipes conveying pulsating fluid. Journal of Sound and Vibration 107, 215–230.

Chen, S.S., 1971. Dynamic stability of a tube conveying fluid. ASME Paper No.71-Vibr.-39.

Ginsberg, J.H., 1973. The dynamic stability of a pipe conveying a pulsatile flow. International Journal of Engineering Science 11, 1013–1024.

Holmes, P.J., 1977. Bifurcations to divergence and flutter in flow induced oscillations: a finite dimensional analysis. Journal of Sound and Vibration 53, 471–503.

Holmes, P.J., 1978. Pipes supported at both ends cannot flutter. Journal of Applied Mechanics 45, 619–622.

Namachchivaya, N.S., 1989. Non-linear dynamics of supported pipe conveying pulsating fluid. 1. Subharmonic resonance. International Journal of Non-linear Mechanics 24, 185–196.

Namachchivaya, N.S., Tien, W.M., 1989a. Non-linear dynamics of supported pipe conveying pulsating fluid. 2.Combination resonance. International Journal of Non-linear Mechanics 24, 197–208.

Namachchivaya, N.S., Tien, W.M., 1989b. Bifurcation behavior of nonlinear pipes conveying pulsating flow. Journal of Fluids and Structures 3, 609–629.

Nayfeh, A.H., Balachandran, B., 1995. Applied Nonlinear Dynamics: Analytical, Computational and Experimental Method. Wiley, New York.

Païdoussis, M.P., 1998. Fluid-Structure Interactions: Slender Structures and Axial Flow, vol. 1. Academic Press, San Diego.

Païdoussis, M.P., Issid, N.T., 1974. Dynamic stability of pipes conveying fluid. Journal of Sound and Vibration 33, 267–294.

Païdoussis, M.P., Issid, N.T., 1976. Experiments on parametric resonance of pipes containing pulsatile flow. Journal of Applied Mechanics 43, 198–202.

Païdoussis, M.P., Sundararajan, C., 1975. Parametric and combination resonances of a pipe conveying pulsating fluid. Journal of Applied Mechanics 42, 780–784.